JOURNAL OF VIROLOGY, June 2004, p. 6102–6111 Vol. 78, No. 12
0022-538X/04/$08.00+0 DOI: 10.1128/JVI.78.12.6102–6111.2004

The *Arabidopsis Cucumovirus Multiplication 1* and *2* Loci Encode Translation Initiation Factors 4E and 4G

Motoyasu Yoshii,[1]†‡ Masaki Nishikiori,[1]† Kayo Tomita,[1] Norimichi Yoshioka,[1] Reiko Kozuka,[1] Satoshi Naito,[1] and Masayuki Ishikawa[1,2]*

Division of Applied Bioscience, Graduate School of Agriculture, Hokkaido University, Sapporo 060-8589,[1] *and CREST, Japan Science and Technology Corporation, Kawaguchi, Saitama 322-0012,*[2] *Japan*

Received 7 October 2003/Accepted 18 February 2004

The *cum1* and *cum2* mutations of *Arabidopsis thaliana* inhibit cucumber mosaic virus (CMV) multiplication. In *cum1* and *cum2* protoplasts, CMV RNA and the coat protein accumulated to wild-type levels, but the accumulation of the 3a protein of CMV, which is necessary for cell-to-cell movement of the virus, was strongly reduced compared with that in wild-type protoplasts. In *cum2* protoplasts, the accumulation of turnip crinkle virus (TCV)-related RNA and proteins was also reduced. Positional cloning demonstrated that *CUM1* and *CUM2* encode eukaryotic translation initiation factors 4E and 4G, respectively. Unlike most cellular mRNA, the CMV RNA lacks a poly(A) tail, whereas the TCV RNA lacks both a 5′-terminal cap and a poly(A) tail. In vivo translation analyses, using chimeric luciferase mRNA carrying the terminal structures and untranslated sequences of the CMV or TCV RNA, demonstrated that these viral untranslated sequences contain elements that regulate the expression of encoded proteins positively or negatively. The *cum1* and *cum2* mutations had different effects on the action of these elements, suggesting that the *cum1* and *cum2* mutations cause inefficient production of CMV 3a protein and that the *cum2* mutation affects the production of TCV-encoded proteins.

Most eukaryotic cellular mRNA has a 5′-terminal cap (m^7GpppN-) and a poly(A) tail, which lead to increased translation efficiency (11; reviewed in references 12 and 29) and increased mRNA stability (reviewed in reference 32). The cap structure serves as the binding site for eukaryotic translation initiation factor 4F (eIF4F). eIF4F consists of two subunits: eIF4E cap-binding subunit and eIF4G (reviewed in reference 14). In plants, an isoform of eIF4F, designated eIFiso4F, has been identified. eIFiso4F consists of an eIFiso4E cap-binding subunit and eIFiso4G (reviewed in reference 4). In vitro eIF4F promotes the translation of mRNA with stable secondary structures in the 5′ untranslated regions (UTRs) more efficiently than does eIFiso4F (13). Other functional differences between eIF4F and eIFiso4F have also been reported (9, 13, 21, 23). eIF4G and eIFiso4G interact not only with eIF4E and eIFiso4E, respectively, but also with eIF4A, eIF3, and the poly(A)-binding protein. eIF3 recruits the 40*S* ribosomal subunit, whereas eIF4A is a DEAD-box RNA helicase that unwinds the 5′ UTR of mRNA to facilitate binding of the 40*S* ribosomal subunit to the 5′ UTR. After binding to the 5′UTR, the 40*S* ribosomal subunit migrates in a 5′-to-3′ direction to the initiation codon, where the 60*S* ribosomal subunit binds and translation begins (reviewed in references 4 and 14). Through the association of the poly(A) tail, the poly(A)-binding protein, eIF4G, eIF4E, and the 5′ cap, capped, polyadenylated mRNA is circularized (36; reviewed in reference 29). This mRNA circularization is thought to contribute to synergistic translation enhancement by the cap and poly(A) structures.

The mRNAs of many RNA viruses lack either the 5′ cap, the 3′ poly(A) tail, or both, but they are stable and efficiently translated in the cytoplasm of host cells through mechanisms that have evolved for each virus (reviewed in reference 12). For example, the genomic RNAs of cucumber mosaic virus (CMV), tobacco mosaic virus (TMV), and brome mosaic virus have a 5′ cap but lack a 3′ poly(A) tail, and their 3′ UTRs contain, instead, tRNA-like structures. The 3′ UTRs of the TMV and brome mosaic virus RNAs contain sequence elements that increase translation efficiency (10, 20; reviewed in reference 12). The genomic RNAs of some plant viruses, including barley yellow dwarf virus (BYDV), turnip crinkle virus (TCV), tomato bushy stunt virus, and satellite tobacco necrosis virus, are uncapped and nonpolyadenylated (1, 7, 25, 37). The translation of BYDV RNA depends strongly on a cap-independent translation enhancer (TE) sequence in the 3′ UTR, and eIF4F is involved in this 3′ TE-enhanced translation in vitro (35). The 5′ UTR of the BYDV RNA is also necessary for the 3′ TE to function (35). TCV, tomato bushy stunt virus, and satellite tobacco necrosis virus RNAs also contain cap-independent TEs in their 3′ UTRs, and their 5′ UTRs are also necessary for efficient translation, at least for the TCV and satellite tobacco necrosis virus RNAs (7, 25, 37).

Virus multiplication depends on the host translation system and many other host functions. The loss of one such host factor results in resistance to the virus. The resistance is expected to be genetically recessive in this case. In fact, several wild-type genes corresponding to recessive mutations that confer resistance to viruses have been identified, and it is thought that they are required for viral multiplication (34, 38). For example, recessive genetic traits of independent plant species that confer resistance against potyviruses have turned out to correspond to

* Corresponding author. Mailing address: Plant Physiology Department, National Institute of Agrobiological Sciences, Tsukuba 305-8602, Japan. Phone: 81-29-838-7440. Fax: 81-29-838-7469. E-mail: ishika32@affrc.go.jp.

† M.Y. and M.N. contributed equally to this work.

‡ Present address: Molecular Genetics Department, National Institute of Agrobiological Sciences, Tsukuba 305-8602, Japan.

mutations in genes encoding eIFiso4E or eIF4E (9, 21, 23, 27). Several lines of experimental evidence indicate that eIFiso4E or eIF4E plays an important, but as yet unrevealed, role in potyvirus infection by interacting with VPg, a small polypeptide covalently attached to the 5′ terminus of the potyvirus RNA (30).

Two recessive mutations of *Arabidopsis thaliana*, *cucumovirus multiplication 1* (*cum 1*) and *cum2*, each reduce the accumulation of CMV in plants. Since they do not drastically affect the multiplication of CMV RNA in protoplasts, it has been suggested that the *cum1* and *cum2* mutations inhibit the cell-to-cell movement of CMV (39, 40). Comparison of the multiplications of a crucifer-infecting tobamovirus (TMV-Cg) and TCV, which belong to different genera (*Tobamovirus* and *Carmovirus*, respectively), with that of CMV (genus *Cucumovirus*) revealed that these mutations do not affect the multiplication of TMV-Cg but that the *cum2* mutation does affect the multiplication of TCV (39, 40). Here, we report that the *CUM1* and *CUM2* genes encode eIF4E and eIF4G, respectively.

MATERIALS AND METHODS

Plants and viruses. *A. thaliana* (L.) Heynh ecotypes Columbia (Col-0) and Landsberg *erecta* (Ler) were used as wild-type ecotypes. The *cum1* and *cum2* mutants are in the Col-0 background (39, 40). CMV-Y, TCV-B, and TMV-Cg were described by Yoshii et al. (39).

Mapping and identification of the *cum1* and *cum2* mutations. The *cum1* and *cum2* mutations were mapped by using 1750 and 1958 F_2 plants, respectively, which were generated by genetic crosses between the respective mutants (Col-0 background), and Ler wild-type plants (details are available on request). The *CUM* genotypes of F_2 plants were determined by measuring the accumulation of viral coat proteins (CPs) in 10 to 18 F_3 plants for each F_2 plant. In some cases, the *CUM* genotypes were confirmed in the F_4 generation. The cleaved amplified polymorphic sequence (CAPS) markers g4539, AG, and GL1; the simple sequence length polymorphism marker nga112; and the restriction fragment length polymorphism marker mi32 have been described by the Arabidopsis Information Resource (http://www.arabidopsis.org). The yeast artificial chromosomes (YACs) EW2E9, EW8D1, and CIC1E8L and the bacterial artificial chromosomes (BACs) F15J5 and F27H5 were obtained from the Arabidopsis Biological Resource Center at Ohio State University. The restriction fragment length polymorphism markers EW2E9L, EW8D1L, and CIC1E8L were prepared from the corresponding YACs by using the thermal asymmetric interlaced-PCR method (22). Restriction digestion with EcoRV, AccII, and AccI was used to generate polymorphic fragments between Col-0 and Ler for EW2E9L, EW8D1L, and CIC1E8L, respectively. The CAPS markers T2O9DraI and F27H5HaeIII were created based on the genomic sequence information for Col-0 and Ler in the Arabidopsis Information Resource. Digestion of PCR products obtained by using primer sets 5′-GGGCCCTATTTCGACATTTT-3′ and 5′-TCGGAAATC GTTCCTGTTTC-3′ for T2O9DraI and 5′-GGCAACATGGAAGCTAGTTCC ATTGGTATACC-3′ and 5′-GATGGAAGAAATAGGGCTGTCTCGAAG-3′ for F27H5HaeIII with DraI and HaeIII, respectively, generated polymorphic DNA fragments between Col-0 and Ler.

To find the *cum1* and *cum2* mutations, 1- to 2-kbp DNA fragments were amplified from the mapped regions of the respective mutant genomic DNA by PCR with specific primers designed from the wild-type (Col-0) sequence in the Arabidopsis Information Resource, purified from gels, and directly sequenced by using a 377 DNA sequencer (Applied Biosystems) and a BigDye terminator sequencing kit (Perkin-Elmer). Information on the primers used to sequence the mutant genomes is available on request. The mutant genome sequences were compared with the wild-type sequence in the database to find base substitutions. The wild-type nucleotides at the candidate mutation sites were confirmed by direct sequencing of relevant DNA fragments that were amplified from the wild-type genomic DNA by PCR.

Complementation analysis of the *cum1* and *cum2* mutations. The T-DNA clone pRK-1 was constructed by subcloning the 6.5-kb XbaI fragment from the BAC F15J5 into the pCLD04541 vector (GenBank accession no. AF184978). The T-DNA clone pKT-1 was constructed by subcloning the 15-kb SpeI fragment from the BAC F27H5 into the pCLD04542 vector. T-DNA clones were electroporated into *Agrobacterium tumefaciens* C58C1 (pGV2260), and these strains were used to transform *A. thaliana* plants by the vacuum infiltration method (2). To confirm that the entire T-DNA fragments were integrated into the mutant genomes, the junction regions between each insert DNA and the cloning site were amplified with the specific primer sets.

Determination of the *CUM1* and *CUM2* mRNA sequences. The entire sequences of the *CUM1* and *CUM2* mRNAs were determined by 5′ and 3′ rapid amplification of cDNA ends with a SMART PCR cDNA synthesis kit (Clontech) and a CAP site cDNA kit (Nippon Gene), followed by DNA sequencing.

Antisera and quantification of viral proteins. cDNA fragments corresponding to subregions of the CMV-Y 1a protein (amino acids 473 to 748) and the TMV-Cg 130,000-molecular-weight (130K) protein (amino acids 643 to 1103) were cloned into the pGEX5X-1 (Amersham-Pharmacia) and pET16b (Novagen) vectors, respectively. For CMV-Y 3a, TMV-Cg 30K, and TCV-B p28, the entire coding regions were cloned into the pET3b (Novagen), pGEX6P-1 (Amersham-Pharmacia), and pET-32c (Novagen) vectors, respectively. Expression, protein purification, and production of rabbit antiserum for the TMV-Cg 130K fusion protein were performed as described for the anti-TMV-L 130K protein serum by Hagiwara et al. (16). The other fusion proteins were expressed in *Escherichia coli* BL21 strains (Novagen) as inclusion bodies, purified by sodium dodecyl sulfate-polyacrylamide gel electrophoresis, eluted from polyacrylamide gel slices, and injected into rabbits. Rabbit antiserum against TMV-Cg CP was prepared by using gel-purified CP from virus particles. Rabbit antisera against CMV-Y 2a, the CMV-D virion, and the TCV-M virion were obtained from C. Masuta, (American Type Culture Collection, Manassas, Va.) and A. E. Simon, respectively. Mouse antiserum against TCV p8 was obtained from T. J. Morris. Immunoblot analysis was performed with the ECL Plus Western Blotting System (Amersham-Pharmacia) according to the manufacturer's instructions.

In vivo translation assay. DNA fragments corresponding to the 5′ UTRs of RNA3 and RNA4 were PCR amplified from an infectious clone for CMV-Y RNA3 obtained from C. Masuta, using primer sets 5′-GGGGTACCGTAATC TAACCACCTGTGTGT-3′–5′-CATGCCATGGAACCTTGGAAAGCCATG CCTCG-3′ and 5′-GGGGTACCGTTATTGTCTACTGACTATATAGA-3′–5′-CATGCCATGGATTCAGATTTGTCCATGACTCGA-3′, respectively. The PCR products were digested with KpnI and NcoI (sites are underlined in the primer sequences) and subcloned between the corresponding restriction sites of the pSP-*luc*+ vector (Promega) to obtain pMP-5′ and pCP-5′. From the pSP-*luc*+ vector, the AatII-XbaI fragment containing the SP6 promoter, the 5′ UTR, and the *luc*+ coding region was transferred to the corresponding AatII-XbaI region of the pSP64Poly(A) vector (Promega) to obtain pV-*luc*+. DNA fragments corresponding to the 3′ UTRs of CMV-Y RNA3 and RNA4 were amplified from the infectious clone of CMV-Y RNA3 by PCR with the forward primers 5′-GCTCTAGACACTTTGGTGCGTATTAGTAT-3′ and 5′-GCTCT AGATTCCGTGTTCCCAGAATCCTCCCTCCGATC-3′, respectively, and the reverse primer 5′-CCGGAATTCTGGTCTCCTTTTGGAGGCCCCCACGAA-3′. The fragments were digested with XbaI and EcoRI (sites are underlined in the primer sequences) and were cloned between the corresponding restriction sites of the pSP-*luc*+ vector to create pMP-3′ and pCP-3′. The XbaI-EcoRI fragments of pMP-3′ or pCP-3′ containing the 3′ UTR sequences were introduced into pMP-5′ or pCP-5′ by using the corresponding restriction sites to create pMP-5′+3′, pCP-5′+3′, or pMP-5′+CP-3′.

cDNA fragments of the 5′ and 3′ portions of the TCV-B genomic RNA (nucleotides 1 to 90 and 2247 to 4050 of the sequence under GenBank accession no. M22445 [5]) were amplified from TCV-B virion RNA by reverse transcription-PCR with the specific primer sets 5′-CGGGGTACCGGTAATCTGCAA ATCCCTGCA-3′–5′-CATGCCATGGCTGTGTTGAGTGTGTGTAGAAG-3′ and 5′-CCGCTCGAGGGTTCGGCTACACTCCAGA-3′–5′-GATCCCCGGG CAGGCCCCCCCCCCGCG-3′, respectively. The PCR products were digested with KpnI plus NcoI and XhoI plus SmaI (the sites are underlined in the primer sequences) and inserted between the corresponding restriction sites of the pV-*luc*+ and pGEM7Zf(+) vectors to obtain p28/88-5′ and pTCV-B1, respectively. The pTCV-B1 sequence differed from the sequence under GenBank accession no. M22445 at nine positions (details are available on request). A DNA fragment corresponding to the 5′ UTR of TCV subgenomic RNA2 (nucleotides 2605 to 2769) was amplified by PCR from pTCV-B1 by using the primer set 5′-CGGG GTACCGGTAATATATGCTTTCTACAACTCTCTC-3′ and 5′-CATGCCA TGGACTTCCGGACTCTAGGATCATT-3′. The PCR product was digested with KpnI and NcoI (the sites are underlined in the primer sequences) and cloned between the corresponding restriction sites of pV-*luc*+ to obtain p38-5′. DNA fragments corresponding to the 3′ UTR of the TCV genomic RNA (nucleotides 2390 to 4050) and subgenomic RNA2 (nucleotides 3798 to 4050) were prepared by PCR with the forward primers 5′-GCTCTAGAGCGACAGCGAC GCAACAG-3′ and 5′-GCTCTAGATACGGTAATAGTGTAGTCTTCTCAT CT-3′, respectively, and the M13 reverse primer of the sequence 5′-CAGG

AAACAGCTATGAC-3′. PCR products were digested with XbaI (the site is underlined in the primer sequences) and SmaI (present in the multicloning site) and inserted between corresponding restriction sites in the pV-*luc*+ vector to obtain p28/88-3′ and p38-3′. The XbaI-SmaI TCV 3′ UTR fragments were also inserted between the corresponding restriction sites of p28/88-5′ and p38-5′ to obtain p28/88-5′+3′ and p38-5′+3′, respectively. The *Renilla* luciferase (RLUC) plasmid, a derivative of pSP64Poly(A), was described by Chiba et al. (6).

Uncapped and capped RNAs were synthesized from linearized plasmids by using the RiboMax (Promega) and AmpliCap (Epicentre Technologies, Madison, Wis.) kits, respectively. Preparation of protoplasts and RNA transfection were carried out essentially as described by Yoshii et al. (39). Briefly, 1.0×10^6 protoplasts were electroporated with 20 pmol each of firefly luciferase (FLUC) and RLUC RNAs at 475 V/cm with a capacitance of 1,000 μF. Protoplasts were cultured at 23°C for 6 h in darkness and harvested. FLUC and RLUC activities were measured by using a dual-luciferase reporter assay system (Promega). RLUC activity per milligram of protein in *cum1* protoplasts was significantly lower than that in wild-type protoplasts ($P < 0.05$ by Student's paired *t* test; approximately 70% of the wild-type level), while RLUC activity in *cum2* protoplasts was similar to that in wild-type protoplasts. Each electroporation was repeated at least three times with protoplasts that were prepared independently.

To determine the genotype of the *cum1* locus, the 400-bp PCR fragment, amplified from the genomic DNA by using primers 5′-TTGGGGAAGTTCCT TGCGACCCG-3′ and 5′-AGTCATCACGAAAGTGTTTGCTCAAAT-3′, was digested with MnlI. The fragment derived from the wild-type (Col-0) genome was cleaved into 258-, 94-, 37-, and 11-bp fragments, while the fragment from the *cum1* genome was cleaved into 258-, 105-, and 37-bp fragments. To determine the genotype of the *cum2* locus, the 1,445-bp PCR fragment, amplified from the genomic DNA by using primers 5′-CCTCCTAAAGTTTGCAGACCTGTG-3′ and 5′-TGTCATCAAATCGAATGTCCTGATTACT-3′, was digested with HaeIII. The fragment derived from the wild-type (Col-0) genome was cleaved into 1,213- and 232-bp fragments, while the fragment from the *cum2* genome was not digested with HaeIII.

Nucleotide sequence accession numbers. The nucleotide sequences of the *CUM1* and *CUM2* mRNAs have been deposited in the GenBank database (accession no. AB107249 and AB107250).

RESULTS

Map-based cloning of *CUM1* and *CUM2*. The *cum1* mutation was previously mapped between CAPS markers g4539 and AG on *A. thaliana* chromosome IV (39). Further fine mapping analyses located the *cum1* mutation within a 65-kb region between DNA markers EW8D1L and EW2E9L (Fig. 1A and B). Determination of an 11-kb sequences within the 65-kb region of the *cum1* genome and comparison with the corresponding wild-type sequences identified a single-base substitution of G to A within the coding region of the *At.EIF4E1* (At4g18040) gene encoding eIF4E (26) (GenBank accession no. AB107250). This base substitution changes the 99th tryptophan codon to a nonsense codon (Fig. 1D).

To confirm that the G-to-A substitution resulted in the *cum1* phenotype, the T-DNA clone pRK-1, which harbors the complete *At.EIF4E1* gene (Fig. 1C), was stably transformed into the *cum1* mutant. Restoration of CMV CP accumulation was observed in inoculated leaves of pRK-1-transformed *cum1* mutants (Fig. 1E). No such restoration was observed in *cum1* plants transformed with a wild-type genomic DNA fragment that overlaps the pRK-1 insert but does not contain the complete *At.EIF4E1* gene (data not shown). The *cum1* mutation was also complemented by the introduction of *At.EIF4E1* cDNA under the control of the cauliflower mosaic virus 35S RNA promoter (data not shown). These results demonstrate that *CUM1* encodes eIF4E.

The *cum2* mutation was previously mapped between DNA markers GL1 and nga112 on *A. thaliana* chromosome III (40). Further fine mapping analyses located the *cum2* mutation in an 80-kb region between DNA markers T2O9DraI and F27H5HaeIII (Fig. 2A and B). Determination of a 45-kb sequence within the 80-kb region of the *cum2* genome and comparison with the corresponding wild-type sequences identified a single-base substitution of C to T within the coding region of the gene encoding eIF4G (At3g60240) (Fig. 2D). Reverse transcription-PCR and 5′ and 3′ rapid amplification of cDNA ends showed that the *eIF4G* gene contains nine exons and the corresponding mRNA contains 5,451 nucleotides [with the exception of a poly(A) tail] and an open reading frame that encodes a polypeptide of 1,725 amino acids (Fig. 2D). In the *cum2* mutant, the 1,327th proline codon is replaced with a serine codon.

To confirm that the C-to-T substitution results in the *cum2* phenotype, the T-DNA clone pKT-1, which harbors the complete *eIF4G* gene (Fig. 2C), was stably transformed into the

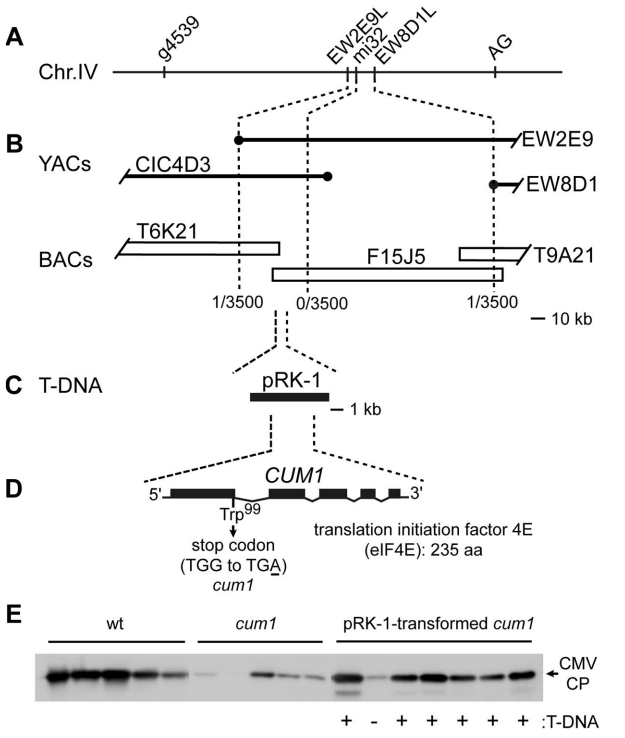

FIG. 1. Map-based cloning of *CUM1*. (A) Map around the *CUM1* locus on chromosome IV (not drawn to scale). DNA markers are indicated above the chromosome. (B) YAC and BAC contiguous DNA sequences encompassing the *CUM1* locus. Circles represent the YAC end probes used for mapping. The numbers of chromatids recombined between the marker and the *CUM1* locus per the numbers of chromatids examined are shown. (C) Position of the T-DNA clone pRK-1, which was tested for complementation ability. (D) Exon-intron structure of the *CUM1* gene, which encodes eIF4E, and location of the *cum1-1* mutation. Filled boxes represent exons, and diagonal lines represent introns. aa, amino acids. (E) Complementation of the *cum1-1* mutation by the T-DNA clone pRK-1. T2 plants derived from a single representative pRK-1-transformed *cum1-1* mutant plant, wild-type Col-0 plants (wt), and *cum1-1* mutant plants were inoculated with CMV-Y. At 48 hpi, inoculated leaves were collected for immunoblotting analysis to assess the accumulation of the CMV-Y CP. Each lane represents one independent plant. The position of the CMV-Y CP is indicated to the right. The presence (+) or absence (−) of the T-DNA insert in each T2 plant is indicated at the bottom.

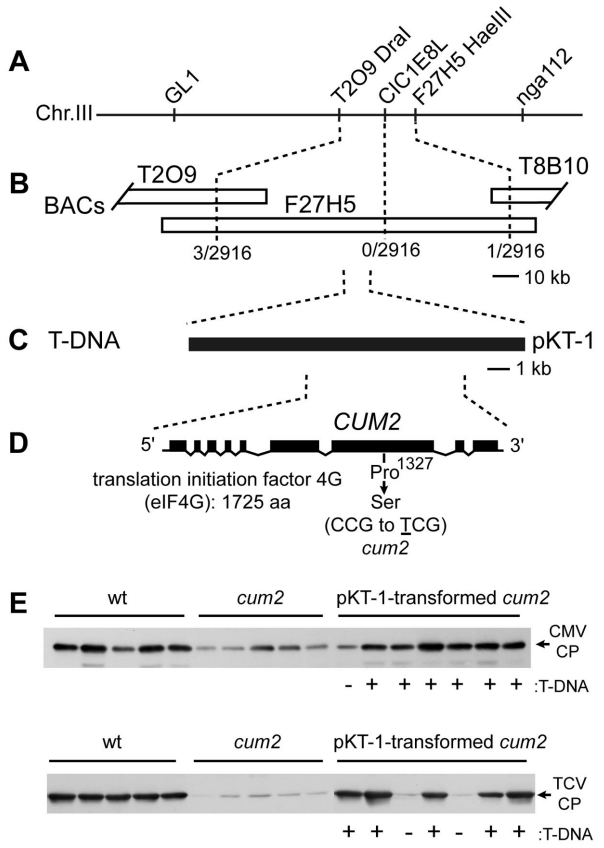

FIG. 2. Map-based cloning of *CUM2*. (A) Map around the *CUM2* locus on chromosome III (not drawn to scale). DNA markers are indicated above the chromosome. (B) BAC contiguous DNA sequence that covers the *CUM2* locus. Open boxes represent BAC clones. The numbers of chromatids recombined between the marker and the *CUM2* locus per the numbers of chromatids examined are shown below the BACs. (C) Position of the T-DNA clone pKT-1, which was tested for complementation ability. (D) Exon-intron structure of the *CUM2* gene, which encodes eIF4G, and location of the *cum2-1* mutation. Filled boxes represent exons, and diagonal lines represent introns. aa, amino acids. (E) Complementation of the *cum2-1* mutation by the T-DNA clone pKT-1. T2 plants derived from a single, representative pKT-1-transformed *cum2-1* mutant plant, the wild-type Col-0 plants (wt), and *cum1-1* mutant plants were inoculated with CMV-Y or TCV-B. At 48 hpi, inoculated leaves were collected for immunoblotting analysis to assess the accumulation of the CMV-Y and TCV-B CPs. Each lane represents one independent plant. The positions of the CMV-Y and TCV-B CPs are indicated to the right. The presence (+) or absence (−) of the T-DNA insert in each T2 plant is indicated at the bottom.

cum2 mutant. Inoculation of leaves of pKT-1-transformed *cum2* mutants with CMV or TCV led to accumulation of the CPs of these viruses to wild-type levels (Fig. 2E). Accumulation of the CPs was not observed in *cum2* plants that were transformed with a wild-type genomic DNA fragment that overlaps the pKT-1 insert but does not contain the complete *eIF4G* gene (data not shown). These results suggest that the C-to-T mutation in the *eIF4G* gene inhibits the multiplication of both CMV and TCV. Similarly, plants that are homozygous for T-DNA insertions in the *eIF4G* gene display reduced multiplication of CMV and TCV, as in the *cum2* mutant (data not shown).

Reduced accumulation of CMV 3a movement protein in mutant protoplasts. CMV accumulation is delayed in *cum1* and *cum2* mutant leaves (39, 40). In protoplasts of these mutants, however, the accumulation patterns of CMV-related RNA and its CP are similar to those in wild-type Col-0 protoplasts (39, 40). To understand how the *cum1* and *cum2* mutations delay CMV accumulation in plants, we further investigated the effect of these mutations on CMV-encoded protein accumulation.

CMV encodes five proteins. Proteins 1a and 2a are involved in viral RNA replication and are synthesized by the translation of CMV RNA1 and RNA2, respectively. Protein 3a is involved in viral cell-to-cell movement and is synthesized by the translation of RNA3. Protein 2b, which suppresses gene silencing, and the CP are synthesized by the translation of the RNA2-derived subgenomic RNA4A and the RNA3-derived RNA4, respectively (Fig. 3A) (3, 8, 24). CMV RNA multiplication from 4 to 8 h postinoculation (hpi) and CP accumulation in *cum1* and *cum2* mutant protoplasts were similar to those in wild-type protoplasts (Fig. 4A), confirming published results (39, 40). As with the CMV CP, the accumulation of the 1a and 2a replication proteins in *cum1* and *cum2* mutant protoplasts was similar to that in wild-type protoplasts (Fig. 4A). In contrast, in *cum1* and *cum2* mutant protoplasts, 3a accumulation was only 20% (ranging from 6 to 64% of wild-type levels in seven independent experiments) and 30% (ranging from 16 to 67% of wild-type levels in six independent experiments) of that in wild-type protoplasts, respectively, at 8 hpi (Fig. 4A and data not shown). These results demonstrate that the *cum1* and *cum2* mutations affect protein 3a accumulation but not the accumulation of CMV RNA3, suggesting that the mutations affect the translation of CMV RNA3 or the stability of the 3a protein.

The *cum1* and *cum2* mutations affect the expression of proteins encoded by RNA carrying noncoding sequences of CMV RNA3. Since eIF4E and eIF4G are involved in translation

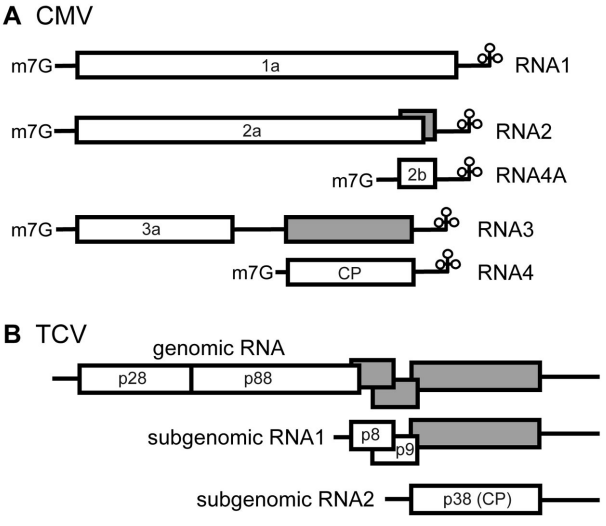

FIG. 3. Structures of the CMV and TCV genomes. ORFs indicated by white boxes are translated, and those indicated by gray boxes are not translated. Note that CMV RNAs are 5′ capped, whereas TCV RNAs are not, and that neither viral RNA is polyadenylated.

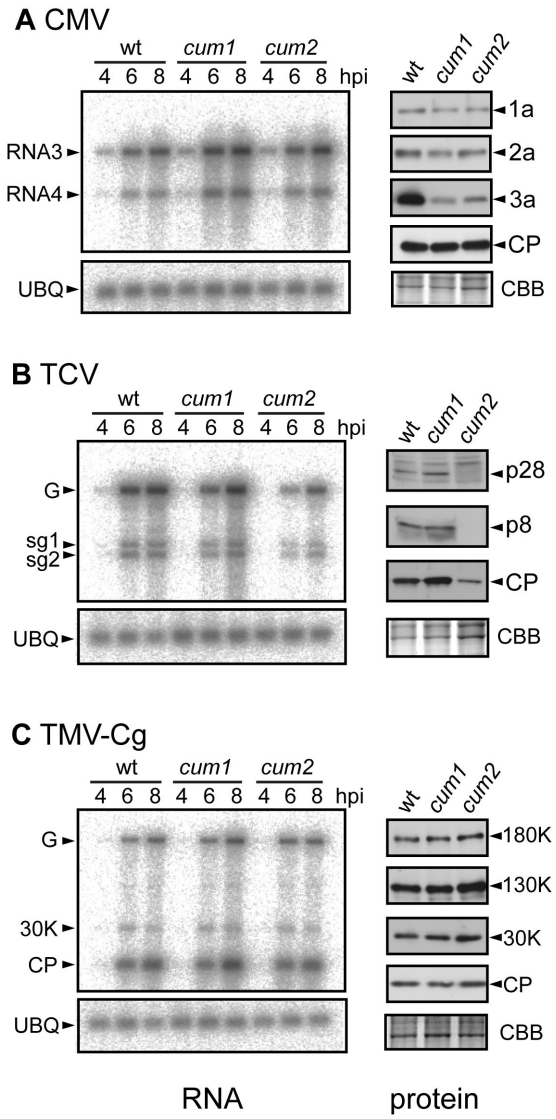

FIG. 4. Accumulation of CMV-, TCV-, and TMV-encoded proteins and RNA in *cum1* and *cum2* mutant and wild-type protoplasts. Protoplasts were prepared from liquid-cultured calli derived from seedlings of Col-0 wild-type (wt) and the *cum1* and *cum2* mutants. Protoplasts (4×10^6) were electroporated with either 7 μg of CMV-Y RNA, 5 μg of TCV RNA, or 20 μg of TMV-Cg RNA. Inoculated protoplasts were cultured for 4, 6, or 8 h for RNA analysis or for 8 h for protein analysis. The accumulation of CMV-Y RNA3, CMV-Y RNA4, and the TMV-Cg- and TCV-M-related RNAs was analyzed by Northern blot hybridization as described by Yoshii et al. (39). RNA bands were visualized with a Bio Imaging analyzer (BAS 1000; Fuji Photo Film, Tokyo, Japan). The accumulation of the virus-encoded proteins was analyzed by immunoblotting as described previously (39). Mock-inoculated wild-type protoplasts were simultaneously analyzed to identify plant-derived RNA and protein bands (data not shown). To confirm that similar amounts of RNA and protein were loaded in each lane, detection of ubiquitin mRNA (UBQ) and Coomassie brilliant blue staining of sodium dodecyl sulfate-polyacrylamide gels (CBB) were performed. (A) Accumulation of CMV-Y-related molecules. Positions of RNA3, RNA4, 1a, 2a, 3a, and the CP are indicated. (B) Accumulation of TCV-B-related molecules. Positions of the genomic RNA (G), subgenomic RNA1 (sg1), subgenomic RNA2 (sg2), and the proteins p28, p8, and the CP are indicated. (C) Accumulation of TMV-Cg-related molecules. Positions of the genomic RNA (G), the 30K and CP subgenomic RNAs, and the 180K, 130K, and 30K proteins and the CP are indicated.

initiation, less efficient RNA3 translation may explain the strong reduction in 3a accumulation in the *cum1* and *cum2* mutant protoplasts. To test this possibility, capped mRNAs of FLUC containing either the 5′ UTR, 3′ UTR, or both UTRs of either CMV RNA3 or RNA4 were constructed because the UTRs of many viral mRNAs contain RNA sequence elements controlling translation efficiency (12). These chimeric FLUC RNAs were synthesized by in vitro transcription and electroporated into *cum1*, *cum2*, and wild-type protoplasts. The internal control, a capped RLUC RNA that carried 5′ and 3′ UTRs derived from an *E. coli* plasmid vector and a 3′ poly$(A)_{30}$, was mixed with the FLUC RNA on electroporation and was used to correct for differences in general translation activity, protoplast quality, and electroporation efficiency. Six hours after electroporation, the cells were harvested and disrupted, and FLUC and RLUC activities were measured.

When capped FLUC RNAs carrying the 3′ UTRs of CMV RNA3 (construct V-3) and RNA4 (construct V-4) were electroporated into the wild-type protoplasts, the relative FLUC activities (the FLUC/RLUC ratios) were 50- and 100-fold higher, respectively, than the relative FLUC activity from FLUC RNA that did not contain any CMV RNA sequences (construct V+) (Table 1). This suggests that the 3′ UTRs of CMV RNA3 and RNA4 harbor elements that enhance the expression of encoded proteins. The relative FLUC activities expressed from V+ RNA in *cum1* and *cum2* protoplasts were not significantly different from that in wild-type protoplasts. In the *cum1* and *cum2* mutant protoplasts, however, the relative FLUC activities from V-3 RNA were significantly lower than that in the wild-type protoplasts (56 and 39% of the wild-type level, respectively). Similarly, the relative FLUC activities from V-4 RNA were significantly lower in the *cum1* and *cum2* mutants than in the wild-type protoplasts (42 and 32% of the wild-type level, respectively) (Table 1). Therefore, the *cum1* and *cum2* mutations each affected the function of the CMV 3′UTRs, which enhanced the expression of encoded proteins.

When capped FLUC RNAs carrying the 5′ UTR of RNA3 and 3′ UTR of RNA3 or RNA4 (construct 3-3 or 3-4) were used for electroporation, the relative FLUC activities expressed in the *cum1* and *cum2* protoplasts were significantly lower than the activity in the wild-type protoplasts (for 3-3, 20 and 9% of the wild-type level, respectively; for 3-4, 19 and 17% of the wild-type level, respectively) (Table 1). The reductions in relative FLUC activity by the *cum1* and *cum2* mutations were greater for constructs 3-3 and 3-4 than for V-3 and V-4. Conversely, when capped FLUC RNA carrying both the 5′ and 3′ UTRs of CMV RNA4 (construct 4-4 in Table 1) was electroporated, the relative FLUC activities expressed in the *cum1* and *cum2* protoplasts were significantly lower than that in the wild-type protoplasts (58 and 43% of the wild-type level in *cum1* and *cum2* protoplasts, respectively). However, the reductions in the relative FLUC activity by the *cum1* and *cum2* mutations were similar to, or even smaller than, that for the construct V-4 (Table 1). These results suggest that the 5′ UTR sequence of CMV RNA3, but not that of RNA4, reduces the relative FLUC activity more drastically in the *cum1* and *cum2* protoplasts than in the wild-type protoplasts. In summary, the *cum1* and *cum2* mutations affected the expression of protein products from RNA carrying the noncoding sequences of CMV RNA3 more strongly than that from RNA carrying the

TABLE 1. FLUC expression from RNAs harboring UTRs of CMV or TCV RNA, which were electroporated into *cum1*, *cum2*, and wild-type protoplasts

Construct				Protoplast type	Relative FLUC activity (FLUC/RLUC ratio)							
5′ cap	5′ UTR	3′ UTR	RNA name (template)		Expt 1	Expt 2	Expt 3	Expt 4	Expt 5	Expt 6	Expt 7	Avg (% of wt)
+	Vector	CMV RNA3	V-3 (pMP-3′-/*Eco*RI)	wt[a]	2.9×10^{-1}	1.6×10^{-1}	1.9×10^{-1}					2.1×10^{-1}
				cum1	1.5×10^{-1}	9.7×10^{-2}	1.1×10^{-1}					1.2×10^{-1}[b] (56)
				cum2	1.0×10^{-1}	8.8×10^{-2}	6.3×10^{-2}					8.4×10^{-2}[b] (39)
+	Vector	CMV RNA4	V-4 (pCP-3′/*Eco*RI)	wt	5.9×10^{-1}	2.5×10^{-1}	5.4×10^{-1}					4.6×10^{-1}
				cum1	2.9×10^{-1}	1.1×10^{-1}	1.8×10^{-1}					1.9×10^{-1}[b] (42)
				cum2	2.3×10^{-1}	7.9×10^{-2}	1.3×10^{-1}					1.5×10^{-1}[b] (32)
+	CMV RNA3	CMV RNA3	3-3 (pMP-5′+3′/*Eco*RI)	wt	1.9×10^{-1}	1.1×10^{-1}	1.7×10^{-1}					1.5×10^{-1}
				cum1	3.2×10^{-2}	2.6×10^{-2}	3.4×10^{-2}					3.0×10^{-2}[b] (20)
				cum2	1.4×10^{-2}	1.6×10^{-2}	1.2×10^{-2}					1.4×10^{-2}[b] (9)
+	CMV RNA3	CMV RNA4	3-4 (pMP-5′+CP-3′/*Eco*RI)	wt	4.3×10^{-1}	2.4×10^{-1}	3.4×10^{-1}					3.4×10^{-1}
				cum1	6.6×10^{-2}	5.2×10^{-2}	7.0×10^{-2}					6.3×10^{-2}[b] (19)
				cum2	9.0×10^{-2}	3.8×10^{-2}	4.9×10^{-2}					5.9×10^{-2}[b] (17)
+	CMV RNA4	CMV RNA4	4-4 (pCP-5′ + 3′/*Eco*RI)	wt	7.0×10^{-1}	4.0×10^{-1}	6.7×10^{-1}					5.9×10^{-1}
				cum1	3.9×10^{-1}	2.6×10^{-1}	3.9×10^{-1}					3.5×10^{-1}[b] (58)
				cum2	3.5×10^{-1}	2.2×10^{-1}	2.0×10^{-1}					2.6×10^{-1}[b] (43)
+	Vector	Vector	V+ (pV-*luc*+/*Eco*ICRI)	wt				2.4×10^{-3}	1.3×10^{-3}	9.9×10^{-3}		4.5×10^{-3}
				cum1				2.8×10^{-3}	1.8×10^{-3}	4.9×10^{-3}		3.2×10^{-3}[c]
				cum2				5.0×10^{-3}	1.6×10^{-3}	4.2×10^{-3}		3.6×10^{-3}[c]
−	Vector	TCV G	V-G (p28/88-3′/*Sma*I)	wt				8.9×10^{-3}	3.5×10^{-3}	1.6×10^{-2}	8.6×10^{-3}	9.3×10^{-3}
				cum1				1.2×10^{-2}	9.5×10^{-3}	2.0×10^{-2}	9.3×10^{-3}	1.3×10^{-2}[d] (138)
				cum2				3.8×10^{-3}	2.4×10^{-3}	2.9×10^{-3}	4.1×10^{-3}	3.3×10^{-3}[e] (35)
−	Vector	TCV Sg2	V-Sg2 (p38-3′/*Sma*I)	wt				1.3×10^{-2}	5.3×10^{-3}	2.3×10^{-2}	1.7×10^{-2}	1.4×10^{-2}
				cum1				1.6×10^{-2}	8.0×10^{-3}	2.6×10^{-2}	1.4×10^{-2}	1.6×10^{-2}[c]
				cum2				4.8×10^{-3}	3.0×10^{-3}	4.4×10^{-3}	6.0×10^{-3}	4.5×10^{-3}[b] (32)
−	TCV G	TCV G	G-G (p28/88-5′ + 3′/*Sma*I)	wt				2.2×10^{-2}	8.2×10^{-3}	4.4×10^{-2}	1.9×10^{-2}	2.3×10^{-2}
				cum1				4.4×10^{-2}	3.8×10^{-2}	7.3×10^{-2}	3.5×10^{-2}	4.8×10^{-2}[d] (206)
				cum2				1.3×10^{-2}	7.3×10^{-3}	1.0×10^{-2}	8.3×10^{-3}	9.6×10^{-3}[e] (42)
−	TCV Sg2	TCV Sg2	Sg2-Sg2 (p38-5′ + 3′/*Sma*I)	wt				4.5×10^{-2}	1.9×10^{-2}	8.6×10^{-2}	4.1×10^{-2}	4.8×10^{-2}
				cum1				1.2×10^{-1}	1.0×10^{-1}	2.2×10^{-1}	1.0×10^{-1}	1.4×10^{-1}[d] (283)
				cum2				1.6×10^{-2}	1.1×10^{-2}	2.1×10^{-2}	1.7×10^{-2}	1.7×10^{-2}[b] (35)
−	Vector	Vector	V−(pV-*luc*+/*Eco*ICRI)	wt				2.4×10^{-5}	3.6×10^{-5}	3.4×10^{-5}		3.1×10^{-5}
				cum1				2.8×10^{-5}	4.2×10^{-5}	2.6×10^{-5}		3.2×10^{-5}[c]
				cum2				5.6×10^{-5}	3.9×10^{-5}	2.0×10^{-5}		3.8×10^{-5}[c]

[a] wt, wild type.
[b] Statistically significant ($P < 0.05$ by Student's paired *t* test, one-sided test) decrease in the FLUC/RLUC ratio compared with wild-type protoplasts.
[c] Not statistically significant ($P > 0.5$ by Student's paired *t*-test) difference from the value for wild-type protoplasts.
[d] Statistically significant ($P < 0.05$ using Student's paired *t*-test, one-sided test) increase in the FLUC/RLUC ratio, as compared with wild-type protoplasts.
[e] Borderline statistically significant ($P < 0.08$ using Student's paired *t*-test, one-sided test) decrease in the FLUC/RLUC ratio, as compared with wild-type protoplasts.

noncoding sequences of CMV RNA4. This explains, at least partly, why CMV 3a protein accumulation, but not CP accumulation, is significantly reduced in CMV-infected *cum1* and *cum2* protoplasts. Furthermore, because the levels of CMV RNA3 accumulation in CMV-inoculated *cum1* and *cum2* protoplasts were similar to those in CMV-inoculated wild-type protoplasts, the stability of CMV RNA3 is unlikely to be affected by the *cum1* and *cum2* mutations. Therefore, the *cum1* and *cum2* mutations probably affect the translation of CMV RNA3.

Reduced accumulation of TCV-related RNA and proteins in *cum2* protoplasts. To understand how the *cum2* mutation inhibits TCV multiplication in plants, we examined the accumulation levels of TCV-related RNA and TCV-encoded proteins in *cum2* protoplasts. TCV encodes five proteins: p28 and p88 are involved in viral RNA replication and are synthesized by the translation of the genomic RNA, p88 is synthesized by the readthrough of the termination codon of p28, p8 and p9 are involved in viral cell-to-cell movement and are synthesized by the translation of subgenomic RNA1, and p38 is the CP and is synthesized by the translation of subgenomic RNA2 (Fig. 3B) (5, 15). As Fig. 4B shows, the accumulation of TCV-encoded p28, p8, and p38 (CP) at 8 hpi and the increase in TCV-related RNA accumulation from 4 to 8 hpi were reduced in *cum2* protoplasts (lower than 40% of the respective wild-type levels in five to eight independent experiments), but not in *cum1* protoplasts, compared to wild-type protoplasts (Fig. 4B and data not shown). This is inconsistent with the results reported by Yoshii et al. (40). To find a plausible explanation for these conflicting data, we checked the genotypes of the protoplasts by using the CAPS analysis (for details, see Materials and Methods) and found that the *cum2* protoplasts used by Yoshii et al. (40) were heavily contaminated with wild-type or *cum2* heterozygous protoplasts (reference 40 and data not shown). We confirmed that the wild-type, *cum1*, and *cum2* seeds used in this study each had correct genotypes of the *cum1* and *cum2* loci by using the CAPS analysis (for details, see Materials and Methods). Therefore, the accumulation of TCV-related RNA and TCV-encoded proteins is reduced in *cum2* protoplasts. For CMV and TMV, the accumulation of viral RNA and CP in noncontaminated *cum2* protoplasts was similar to that in wild-type protoplasts (Fig. 4A and C).

The *cum2* mutation affects the expression of protein products encoded by RNAs carrying noncoding sequences of TCV RNA. In order to obtain insight into the inhibition mechanisms of TCV multiplication by the *cum2* mutation, we examined the effect of the *cum1* and *cum2* mutations on the expression of protein products encoded by FLUC RNA mimicking the TCV RNA. Since the 5′ terminus of the TCV RNA is naturally uncapped, uncapped FLUC RNAs containing UTRs from TCV genomic RNA or subgenomic RNA2 were prepared. These RNAs were electroporated into the wild-type, *cum1*, and *cum2* protoplasts with the capped RLUC internal control RNA described above, and the expressed FLUC and RLUC activities were determined 6 h after electroporation.

Uncapped FLUC RNA containing the 5′ and 3′ UTR sequences derived from a plasmid vector (construct V−) expressed only low levels of relative FLUC activity. The relative FLUC activities in the *cum1* and *cum2* mutant protoplasts were not significantly different from that in the wild-type protoplasts (Table 1). Replacement of the vector-derived 3′ UTR with the 3′ UTRs of TCV genomic RNA (construct V-G) and subgenomic RNA2 (construct V-Sg2) drastically increased the relative FLUC activity in wild-type protoplasts (Table 1). In the constructs carrying the 3′ UTRs of TCV RNA, replacement of the 5′ UTRs from the vector-derived sequence with that from TCV genomic and subgenomic RNAs (constructs G-G and Sg2-Sg2) further increased the FLUC expression in the wild-type protoplasts (Table 1). These results are consistent with the conclusions of Qu and Morris (25) that the 3′ UTR of TCV RNA contains a major TE and that the 5′ and 3′ UTRs of TCV genomic or subgenomic RNA synergistically enhance translation.

For the constructs containing the TCV 3′ UTRs (V-G, V-Sg2, G-G, and Sg2-Sg2), the relative FLUC expression in *cum2* mutant protoplasts was moderately, but significantly, reduced compared to that in the wild-type protoplasts (32 to 42% of the respective wild-type levels) (Table 1). These results suggest that the *cum2* mutation affects the expression of TCV-encoded proteins. Interestingly, in the *cum1* mutant protoplasts, the relative FLUC expression from constructs V-G, G-G, and Sg2-Sg2 was significantly higher than that in the wild-type protoplasts (Table 1).

DISCUSSION

In this study, we demonstrated that *CUM1* and *CUM2* encode eIF4E and eIF4G, respectively. Inoculation of CMV RNA into the *cum1* and *cum2* mutant protoplasts revealed that the mutations affected 3a protein accumulation but not the accumulation of CMV RNA and the 1a, 2a, and coat proteins (Fig. 4A). Moreover, the expression of protein products from the capped chimeric FLUC RNA carrying the 5′ and 3′ UTRs of CMV RNA3 (construct 3-3 in Table 1) was severely reduced, but the expression from the capped chimeric FLUC RNA carrying the 5′ and 3′ UTRs of CMV RNA4 (construct 4-4 in Table 1) was only mildly affected by the *cum1* and *cum2* mutations. For TCV, the accumulations of viral RNA and proteins were all reduced in TCV-infected *cum2* mutant protoplasts as far as we examined (Fig. 4B). Electroporation experiments with uncapped chimeric FLUC RNA carrying the 3′ UTR of TCV RNA demonstrated that the *cum2* mutation affected the expression of protein products from this RNA (Table 1).

eIF4E- and eIF4G-related genes in *A. thaliana*. The *A. thaliana* genome contains five genes that encode eIF4E-related proteins: eIF4E (CUM1), eIFiso4E (26), a novel cap-binding protein (28), and two eIF4E-like proteins (At1g29550 and At1g29590). At1g29550 and At1g29590 are closely related to eIF4E and are expressed at the mRNA level (Arabidopsis Information Resource [http://www.arabidopsis.org/] and M. Yoshii, R. Kozuka, S. Naito, and M. Ishikawa, unpublished results) but remain to be analyzed further. The presence of these homologs may explain why the loss of eIF4E (CUM1) due to a nonsense mutation is not lethal to *A. thaliana*. Mutations in the *eIF4E* and *eIFiso4E* genes confer resistance against potyviruses in several plant species (9, 21, 23, 27). One of these mutations, *lsp1* in *A. thaliana*, inhibits the multiplication of turnip mosaic virus at the single-cell level, suggesting that eIFiso4E is required for turnip mosaic virus gene expression or

replication (21). However, it is not known whether *lsp1* inhibits the translation of turnip mosaic virus RNA.

The *A. thaliana* genome contains at least three genes that encode eIF4G-related proteins: eIF4G (CUM2) and two eIFiso4G proteins. The two *A. thaliana* eIFiso4G genes (At2g24050 and At5g57870) are expressed at the mRNA level (Arabidopsis Information Resource). In wheat, eIF4E and eIF4G form the eIF4F complex, and eIFiso4E and eIFiso4G form the eIFiso4F complex (4). Since the *cum1* and *cum2* mutations have similar effects on the expression of CMV 3a protein, eIF4F probably has a specialized function in the process, which eIFiso4F or the other eIF4F-like complexes perform less efficiently. The eIF4G protein not only binds to eIF4E but also binds to eIF4A helicase and eIF3, and the *cum2-1* mutation (1,327th Pro to Ser) resides in a region that corresponds to the domain identified to be important for the binding to eIF4A and eIF3 in human eIF4GI (17). Therefore, the *cum2* mutation may affect the binding of eIF4G to eIF4A or eIF3.

Effects of the *cum1* and *cum2* mutations on protein expression from CMV RNA. Inclusion of the 3′ UTRs of CMV RNA3 or RNA4 in capped chimeric FLUC RNA enhanced the relative FLUC expression, and the enhancement conferred by the CMV 3′ UTRs was affected by the *cum1* and *cum2* mutations (Table 1). This suggests that eIF4E and eIF4G are involved in this enhancement and that eIFiso4E and eIFiso4G can carry out this process, albeit less efficiently.

In yeast, mutations in the eIF4E and eIF4G genes that strongly inhibit translation initiation also increase the rate of mRNA deadenylation and decapping, the key steps in a major mRNA decay pathway (31, 32). In addition, in plants, mRNA stability is often correlated with translation (33). Therefore, it is possible that the *cum1* and *cum2* mutations lead to the instability of mRNA carrying CMV UTRs. However, CMV RNA accumulated to wild-type levels in CMV-infected *cum1* and *cum2* mutant protoplasts (Fig. 4A). Therefore, the *cum1* and *cum2* mutations probably affect the translation of RNA carrying the 3′ noncoding sequence of CMV RNA, rather than the stability of this RNA.

Capped, polyadenylated mRNA can be circularized through linkage of the 3′ poly(A) tail, poly(A)-binding protein, eIF4G, eIF4E, and 5′ cap, and this circularization is thought to be important for efficient translation (36; reviewed in reference 29). Therefore, like poly(A) tails, the 3′ UTRs of CMV RNA may interact with the eIF4F complex directly or indirectly, contributing to efficient translation of CMV RNA through circularization of the mRNA.

The presence of a stable secondary structure in the 5′ UTR inhibits translation initiation (18). The 5′ UTR of CMV RNA3 harbors more stable secondary structures than do the 5′ UTRs of CMV RNA1, RNA2, and RNA4 (Fig. 5 and data not shown). It has been reported that chimeric FLUC RNA that contains the CMV RNA3 5′ UTR is translated less efficiently in vitro than mRNA that contains the 5′ UTRs of other CMV RNA segments (19). Consistent with these observations, we showed that FLUC RNA containing the CMV RNA3 5′ UTR expressed less FLUC activity in vivo than that containing the 5′ UTR of CMV RNA4 (FLUC/RLUC ratios of 3.4×10^{-1} and 5.9×10^{-1} for constructs 3-4 and 4-4, respectively [Table 1]).

We also demonstrated that the relative FLUC activity expressed from chimeric RNA carrying the 5′ UTR of RNA3 and the 3′ UTR of RNA3 or RNA4 (construct 3-3 or 3-4 in Table 1) was more severely affected by the *cum1* and *cum2* mutations than that from FLUC RNA carrying only the 3′ UTRs of CMV RNA (constructs V-3 or V-4 in Table 1). This suggests that eIF4F facilitates the in vivo translation of RNA containing the CMV RNA3 5′ UTR, which has a strong secondary structure, more efficiently than does eIFiso4F. In keeping with this possibility, Gallie and Browning (13) demonstrated that eIF4F promotes the in vitro translation of RNA with highly structured 5′ UTRs more efficiently than eIFiso4F does. Therefore, the observed inefficient expression of protein products from CMV RNA3 in the *cum1* and *cum2* mutants probably reflects an additive effect of the independent responses to the mutations, which the 5′ and 3′ UTRs of CMV RNA3 show on translation.

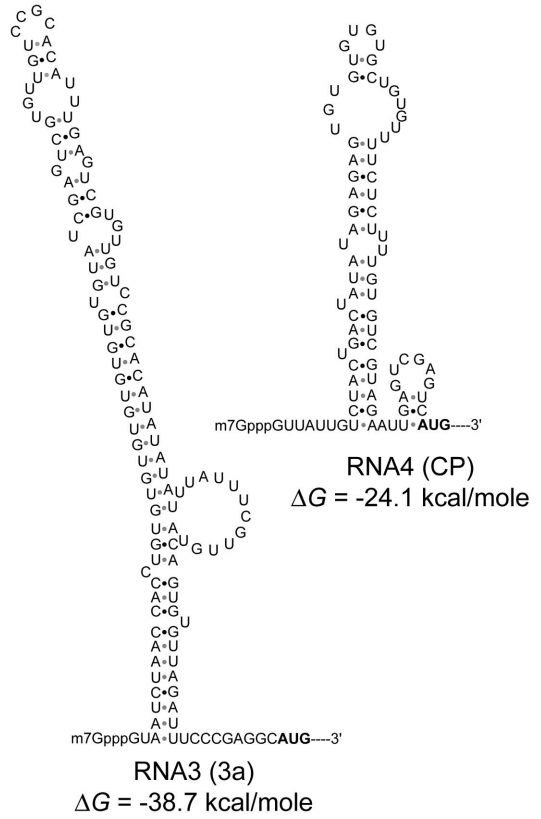

FIG. 5. Predicted secondary structures of the 5′ UTRs of CMV RNA3 and RNA4. Secondary structures were predicted by using MFOLD version 2.3 (41). The free energies (ΔG) of the 5′ UTR structures were calculated by using the default settings and a folding temperature of 23°C.

Effects of the *cum2* mutation on translation of the TCV RNA. Qu and Morris (25) have shown that the genomic RNA of TCV lacks a 5′ cap structure and that the 5′ and 3′ UTRs of the genomic and subgenomic RNAs of TCV enhance their translation. Our results with wild-type protoplasts confirm their conclusions and suggest that the 3′ UTRs of TCV RNA contain a strong cap-independent TE and that the 5′ UTRs of TCV RNA contain a weak cap-independent TE.

The *cum2* mutation affected protein expression from uncapped RNA containing the TCV 3′ UTR (Table 1). This

suggests that enhanced expression of encoded proteins by the 3′ UTR of TCV RNA involves eIF4G. The *cum1* mutation did not adversely affect, and in fact enhanced, the functioning of the 3′ UTR of TCV (Table 1). Therefore, eIF4E is dispensable for this mechanism or may even have an inhibitory effect on the functioning of the 3′ UTR of TCV. Since the enhanced relative FLUC expression conferred by the TCV 3′ UTR still occurs in the *cum2* mutant (compare V-G or V-Sg2 with V− in Table 1), eIFiso4G may carry out this process more weakly, or the *cum2* mutant allele may have residual activity. It has been shown that eIF4F participates in the cap-independent and 3′ TE-dependent translation of BYDV RNA in vitro (35). If a common mechanism underlies the translation of BYDV and TCV RNAs, it is plausible that the *cum2* mutation affects the expression of TCV-encoded proteins via translation inhibition. However, our results alone do not eliminate the possibility that the *cum2* mutation affects the stability of TCV RNA.

The results with CMV suggest that the *cum1* and *cum2* mutations affect the production of the 3a protein and that reduced accumulation of 3a causes delayed CMV multiplication in plants. Similarly, the results with TCV suggest that the *cum2* mutation primarily affects the production of the p28 replication protein of TCV and that reduced accumulation of p28 inhibits the TCV RNA multiplication within a cell and in plants. However, future experiments should carefully test whether the observed phenotypes are in a direct cause-and-effect relationship. In addition, these mutations might alter the expression of many proteins, so that the observed phenotypes of the *cum1* and *cum2* mutants might be caused by alterations in the expression of other host proteins. In fact, eIF4E is overexpressed with the loss of eIFiso4E (9). Therefore, it is possible that eIFiso4E and eIFiso4G are overexpressed to compensate for the loss of eIF4E or eIF4G. The effect of the depletion of eIF4E or eIF4G may be examined more directly by using an in vitro translation system.

ACKNOWLEDGMENTS

We thank D. Shibata, Y.-G. Liu, C. Masuta, T. J. Morris, A. E. Simon, and the Arabidopsis Biological Resource Center for materials and K. Komoda for help with antibody preparation. We also thank D. B. Goto and F. van Werven for careful readings of the manuscript and K. Fujiwara for general assistance.

This work was supported in part by grants from the Japan Society for the Promotion of Science to M.I.

REFERENCES

1. **Allen, E., S. Wang, and W. A. Miller.** 1999. Barley yellow dwarf virus RNA requires a cap-independent translation sequence because it lacks a 5′ cap. Virology **253:**139–144.
2. **Bechtold, N., and G. Pelletier.** 1998. In planta Agrobacterium-mediated transformation of adult *Arabidopsis thaliana* plants by vacuum infiltration. Methods Mol. Biol. **82:**259–266.
3. **Brigneti, G., O. Voinnet, W.-X. Li, L.-H. Ji, S.-W. Ding, and D. C. Baulcombe.** 1998. Viral pathogenicity determinants are suppressors of transgene silencing in *Nicotiana benthamiana*. EMBO J. **17:**6739–6746.
4. **Browning, K. S.** 1996. The plant translational apparatus. Plant Mol. Biol. **32:**107–144.
5. **Carrington, J. C., L. A. Heaton, D. Zuidema, B. I. Hillman, and T. J. Morris.** 1989. The genome structure of turnip crinkle virus. Virology **170:**219–226.
6. **Chiba, Y., R. Sakurai, M. Yoshino, K. Ominato, M. Ishikawa, H. Onouchi, and S. Naito.** 2003. *S*-Adenosyl-L-methionine is an effector in the posttranscriptional autoregulation of the cystathionine gamma-synthase gene in *Arabidopsis*. Proc. Natl. Acad. Sci. USA **100:**10225–10230.
7. **Danthinne, X., J. Seurinck, F. Meulewaeter, M. van Montagu, and M. Cornelissen.** 1993. The 3′ untranslated region of satellite tobacco necrosis virus RNA stimulates translation in vitro. Mol. Cell. Biol. **13:**3340–3349.
8. **Ding, S.-W., B. J. Anderson, H. R. Haase, and R. H. Symons.** 1994. New overlapping gene encoded by the cucumber mosaic virus genome. Virology **198:**593–601.
9. **Duprat, A., C. Caranta, F. Revers, B. Menand, K. S. Browning, and C. Robaglia.** 2002. The *Arabidopsis* eukaryotic initiation factor (iso)4E is dispensable for plant growth but required for susceptibility to potyviruses. Plant J. **32:**927–934.
10. **Gallie, D. R., and V. Walbot.** 1990. RNA pseudoknot domain of tobacco mosaic virus can functionally substitute for a poly(A) tail in plant and animal cells. Genes Dev. **4:**1149–1157.
11. **Gallie, D. R.** 1991. The cap and poly(A) tail function synergistically to regulate mRNA translational efficiency. Genes Dev. **5:**2108–2116.
12. **Gallie, D. R.** 1996. Translational control of cellular and viral mRNAs. Plant Mol. Biol. **32:**145–158.
13. **Gallie, D. R., and K. S. Browning.** 2001. eIF4G functionally differs from eIFiso4G in promoting internal initiation, cap-independent translation, and translation of structured mRNAs. J. Biol. Chem. **276:**36951–36960.
14. **Gingras, A.-C., B. Raught, and N. Sonenberg.** 1999. eIF4 initiation factors: effectors of mRNA recruitment to ribosomes and regulators of translation. Annu. Rev. Biochem. **68:**913–963.
15. **Hacker, D. L., I. T. D. Pretty, N. Wei, and T. J. Morris.** 1992. Turnip crinkle virus genes required for RNA replication and virus movement. Virology **186:**1–8.
16. **Hagiwara, Y., K. Komoda, T. Yamanaka, A. Tamai, T. Meshi, R. Funada, T. Tsuchiya, S. Naito, and M. Ishikawa.** 2003. Subcellular localization of host and viral proteins associated with tobamovirus RNA replication. EMBO J. **22:**344–353.
17. **Imataka, H., and N. Sonenberg.** 1997. Human eukaryotic translation initiation factor 4G (eIF4G) possesses two separate and independent binding sites for eIF4A. Mol. Cell. Biol. **17:**6940–6947.
18. **Kozak, M.** 1986. Influences of mRNA secondary structure on initiation by eukaryotic ribosomes. Proc. Natl. Acad. Sci. USA **83:**2850–2854.
19. **Kwon, C. S., and W.-I. Chung.** 2000. Differential roles of the 5′ untranslated regions of cucumber mosaic virus RNAs 1, 2, 3 and 4 in translational competition. Virus Res. **66:**175–185.
20. **Lahser, F. C., L. E. Marsh, and T. C. Hall.** 1993. Contributions of the brome mosaic virus RNA-3 3′-nontranslated region to replication and translation. J. Virol. **67:**3295–3303.
21. **Lellis, A. D., K. D. Kasschau, S. A. Whitham, and J. C. Carrington.** 2002. Loss-of-susceptibility mutants of *Arabidopsis thaliana* reveal an essential role for eIF(iso)4E during potyvirus infection. Curr. Biol. **12:**1046–1051.
22. **Liu, Y. G., and R. F. Whittier.** 1995. Thermal asymmetric interlaced PCR: automatable amplification and sequencing of insert end fragments from P1 and YAC clones for chromosome walking. Genomics **25:**674–681.
23. **Nicaise, V., S. German-Retana, R. Sanjuan, M.-P. Dubrana, M. Mazier, B. Maisonneuve, T. Candresse, C. Caranta, and O. LeGall.** 2003. The eukaryotic translation initiation factor 4E controls lettuce susceptibility to the potyvirus Lettuce mosaic virus. Plant Physiol. **132:**1272–1282.
24. **Palukatis, P., M. J. Roossinck, R. G. Dietzgen, and R. I. B. Francki.** 1992. Cucumber mosaic virus. Adv. Virus Res. **41:**281–348.
25. **Qu, F., and T. J. Morris.** 2000. Cap-independent translational enhancement of turnip crinkle virus genomic and subgenomic RNAs. J. Virol. **74:**1085–1093.
26. **Rodriguez, C. M., M. A. Freire, C. Camilleri, and C. Robaglia.** 1998. The *Arabidopsis thaliana* cDNAs coding for eIF4E and eIF(iso)4E are not functionally equivalent for yeast complementation and are differentially expressed during plant development. Plant J. **13:**465–473.
27. **Ruffel, S., M.-H. Dussault, A. Palloix, B. Moury, A. Bendahmane, C. Robaglia, and C. Caranta.** 2002. A natural recessive resistance gene against potato virus Y in pepper corresponds to the eukaryotic initiation factor 4E (eIF4E). Plant J. **32:**1067–1075.
28. **Ruud, K. A., C. Kuhlow, D. J. Goss, and K. S. Browning.** 1998. Identification and Characterization of a novel cap-binding protein from *Arabidopsis thaliana*. J. Biol. Chem. **273:**10325–10330.
29. **Sachs, A.** 2000. Physical and functional interactions between the mRNA cap structure and the poly(A) tail, p. 447–465. *In* N. Sonenberg, J. W. B. Hershey, and M. Mathew (ed.), Translational control of gene expression. Cold Spring Harbor Laboratory Press, Cold Spring Harbor, N.Y.
30. **Schaad, M. C., R. J. Anderberg, and J. C. Carrington.** 2000. Strain-specific interaction of the tobacco etch virus NIa protein with the translation initiation factor eIF4E in the yeast two-hybrid system. Virology **273:**300–306.
31. **Schwartz, D. C., and R. Parker.** 1999. Mutations in translation initiation factors lead to increased rates of deadenylation and decapping of mRNAs in *Saccharomyces cerevisiae*. Mol. Cell. Biol. **19:**5247–5256.
32. **Schwartz, D. C., and R. Parker.** 2000. Interaction of mRNA translation and mRNA degradation in *Saccharomyces cerevisiae*, p. 807–825. *In* N. Sonenberg, J. W. B. Hershey, and M. Mathew (ed.), Translational control of gene expression. Cold Spring Harbor Laboratory Press, Cold Spring Harbor, N.Y.
33. **Sullivan, M. L., and P. J. Green.** 1993. Post-transcriptional regulation of nuclear-encoded genes in higher plants: the roles of mRNA stability and translation. Plant Mol. Biol. **23:**1019–1104.
34. **Tsujimoto, Y., T. Numaga, K. Ohshima, M. Yano, R. Ohsawa, D. B. Goto, S.**

Naito, and M. Ishikawa. 2003. Arabidopsis TOBAMOVIRUS MULTIPLICATION (TOM) 2 locus encodes a transmembrane protein that interacts with TOM1. EMBO J. **22:**335–343.
35. **Wang, S., K. S. Browning, and W. A. Miller.** 1997. A viral sequence in the 3′-untranslated region mimics a 5′cap in facilitating translation of uncapped mRNA. EMBO J. **16:**4107–4116.
36. **Wells, S. E., P. E. Hillner, R. D. Vale, and A. B. Sachs.** 1998. Circularization of mRNA by eukaryotic translation initiation factors. Mol. Cell **2:**135–140.
37. **Wu, B., and K. W. White.** 1999. A primary determinant of cap-independent translation is located in the 3′-proximal region of the tomato bushy stunt virus genome. J. Virol. **73:**8982–8988.
38. **Yamanaka, T., T. Ohta, M. Takahashi, T. Meshi, R. Schmidt, C. Dean, S. Naito, and M. Ishikawa.** 2000. TOM1, an *Arabidopsis* gene required for efficient multiplication of a tobamovirus, encodes a putative transmembrane protein. Proc. Natl. Acad. Sci. USA **97:**10107–10112.
39. **Yoshii, M., N. Yoshioka, M. Ishikawa, and S. Naito.** 1998. Isolation of an *Arabidopsis thaliana* mutant in which accumulation of cucumber mosaic virus is delayed. Plant J. **13:**211–219.
40. **Yoshii, M., N. Yoshioka, M. Ishikawa, and S. Naito.** 1998. Isolation of an *Arabidopsis thaliana* mutant in which the multiplication of both cucumber mosaic virus and turnip crinkle virus is affected. J. Virol. **72:**8731–8737. (Author's correction, **77:**8178, 2003.)
41. **Zuker, M.** 2003. Mfold web server for nucleic acid folding and hybridization prediction. Nucleic Acids Res. **31:**3406–3415.